ISSN 1068–3372, Journal of Contemporary Physics (Armenian Academy of Sciences), 2017, Vol. 52, No. 4, pp. 366–374. © Allerton Press, Inc., 2017.
Original Russian Text © S.G. Arutunian, G.S. Harutynyan, D. Choe, M. Chung, E.G. Lazareva, A.V. Margaryan, 2017, published in Izvestiya Natsional'noi Akademii Nauk Armenii, Fizika, 2017, Vol. 52, No. 4, pp. 495–506.

Effects of Scanning Speed on the Laser Beam Profile Measurements by Vibrating Wire

S. G. Arutunian[a], G. S. Harutynyan[a], D. Choe[b], M. Chung[b], E. G. Lazareva[a*], and A. V. Margaryan[a]

[a]*Alikhanyan National Scientific Laboratory, Yerevan, Armenia*
[b]*Ulsan National Institute of Science and Technology, Ulsan, Korea*
[*] *ella.lazareva@yerphi.am*

Received June 14, 2017

Abstract—For measuring laser beam profiles, a vibrating wire monitor (VWM) has been introduced. The measurements were carried out at different speeds of scan. Preliminary estimates were made for the calculation of the VWM response times with respect to the thermal losses along the wire, and radiative and convective losses. These estimates, however, do not determine the difference between the beam profile and the frequency response of the VWM for a given scan rate. To evaluate the reliability of the frequency response of the VWM, comparisons between forward and reverse beam scans at different speeds have been used. The results of these scans are used to correct the thermal inertia in the frequency response of the VWM.

DOI: 10.3103/S1068337217040090
Keywords: vibrating wire monitor, laser beam, oscillation frequency

1. INTRODUCTION

The operating principle of vibrating wire monitor is based on the measurement of the change of the frequency of a vibrating wire, which is stretched on a support, depending on the physical parameters of the wire and environment in which oscillations take place [1−2].

The advantages of the vibrating wire monitors are their long-term stability, high accuracy and resolution, good reproducibility, zero drift, minimal sensitivity change and small hysteresis. The frequency signal is subject to external disturbances only slightly and can be transmitted over a long cable without loss or degradation [3–6]. The change in the tension of the vibrating wire can occur due to a change in the temperature of the wire, which leads to a shift in the frequency of oscillation of the wire. This shift can be caused, in particular, by the passage of a beam of charged particles (radiation) through a wire material and serves as a measure of the flux of particles scattered along the wire [7–9]. Thus, the usable principle of operation is universal for beams of charged particles and for laser beams. We also note the difference between the use of a vibrating wire and the conventional method of using thin wires as targets. The signal for the vibrating wire is formed as a result of measuring the frequency of the vibrating wire and does not require additional means for measuring the scattered charged particles (photons) (compare, for example, with [10]).

The frequency of the vibrating wire monitors (VWM), depending on the initial tension of the string, material and the size of the sensor, is in the range of 1−10 kHz. The typical range of the output signal – frequency shift – is more than 0.01 (lower limit) and less than 1000 Hz (upper limit), that is, a relative dynamic range of $1–10^5$ is achievable. The monitor resolution is ~0.001 Hz, and the measurement accuracy is better than 0.01 Hz. Depending on the wire material and its geometric dimensions, this accuracy corresponds to the accuracy of measuring the wire temperature variation (less than 1 mK). The VWMs were used to measure electron beams [8], proton beams [9, 11–13], ion beams [14], X-ray beams [15], and synchrotron radiation beams [16]. Special monitors with gadolinium-covering wire have been proposed for thermal neutrons beams profiling [17].

Important parameters of the VWM are dynamic characteristics, which are determined by the geometry and material of the monitor, the environment, and the scanning speed.

The aim of the present work is the investigation of the process of measuring the beam profile by the VWM at different scan speeds. This investigation allows to estimate the accuracy of the scan depending on the scan speed. In this work the method of direct and reverse scannings is applied, which allows the correction of the thermal delay of the frequency response of the VWM with increasing the scan speed.

2. TIMING DIAGRAM AND DATA PROCESSING FOR FAST SCAN

The scan of any beam with VWM needs a set of frequency measurements in fixed positions of the wire. The electronic board of the VWM for each wire consists of the two main units: wire oscillation generator (StrinGen) and the frequency measurement unit. The core of this unit is microcontroller PIC18F25×× series. The data transfer to computer is provided via RS232 or USB interface.

The measurement of the wire oscillations frequency F in the time frame g is done by counting of N_q precise quartz generator high frequency F_q periods in N_f numbers of the full wire frequency periods that approximately cover the time gate g (Fig. 1). The wire oscillation periods are fixed precisely by usage of zero-crossing mechanism. From the equality

$$\frac{N_f}{F} = \frac{N_q}{F_q} \approx g \qquad (1)$$

there an equation for the value of the frequency of the vibrating wire is found:

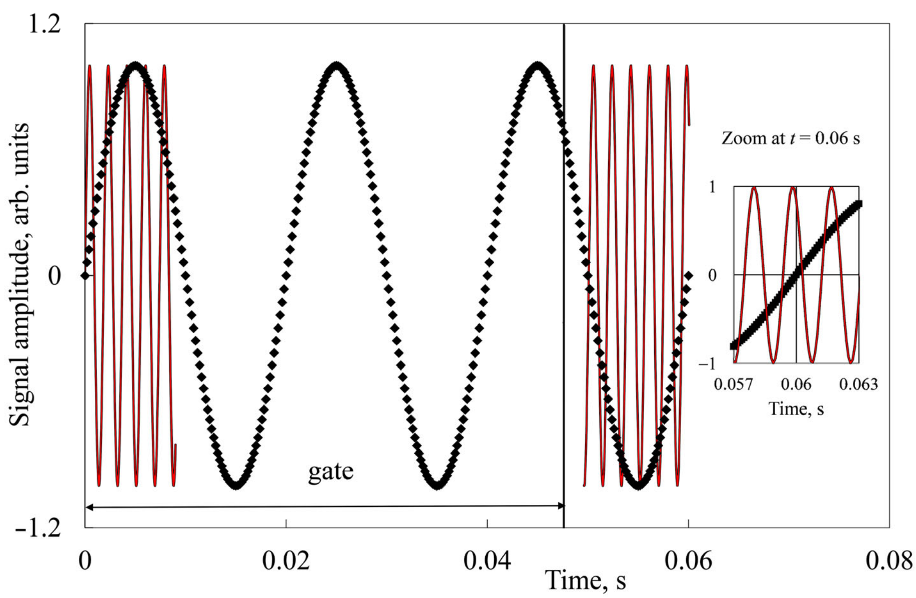

Fig. 1. Principle of wire oscillation frequency measurement: solid line – quartz high frequency, diamonds are frequency signal of the wire, vertical line – preliminary set gate g. In the insert the zoom around t = 0.06 s is presented.

$$F = F_{\mathrm{q}} \frac{N_{\mathrm{f}}}{N_{\mathrm{q}}}. \tag{2}$$

At the end of the time gate the crossing of high frequency can happen at any phase of quartz generator period (see insert in Fig. 1), so the number of quartz periods can vary on one digit. The corresponding accuracy of the method is presented by the following equation

$$\frac{\Delta F}{F} \approx \frac{1}{N_{\mathrm{q}}} \approx \frac{1}{g F_{\mathrm{q}}}. \tag{3}$$

Therefore, the relative accuracy of measurements at 1 s sampling and 1 MHz quartz is $\sim 10^{-6}$.

At fast scan we should take into account detailed information of frequency measurement timing and wire motion processes. Microcontroller PIC18F25×× provides the measurement process and the result is sent to the computer as 4 bytes in floating point format. The computer time $t_{\mathrm{f\_PC}}$ at this information receiving is saved in data file. Actually, this time does not correspond to the real measurement time t_{f} that should be assigned to the middle point of the gate g : $t_{\mathrm{f}} = t_{\mathrm{f\_PC}} - 6.5\ \mathrm{ms} - g/2$. It is considered that the delay between the edge of the gate and the end of the transmission time of the data packet to the computer is ~ 6.5 ms. In the experiment, the value g = 180 ms was used and the gap of 20 ms between the new measurement process start was set for data transfer to the computer (the total cycle time was thus 200 ms). For the RS232 interface, the 9600 Baud rate was used, which corresponds to ~1 ms for 1 byte transfer (including start and stop bits).

The transmitting of the frequency data is followed by request of stepper motor position. Immediately after sending the request, the time of computer is written in the data file, which practically corresponds to the real time of position t_{StM} that will be received in a few ms later. These two columns (t_{StM} and stepper motor positions) are used to calculate in linear approximation the position of motor at frequency measurement time t_{f}. The beam profile measurement is presented as pairs of wire frequency and stepper motor position.

3. MEASUREMENT OF THE LASER BEAM PROFILE

During the experiment, the transverse profile of the laser beam was measured by measuring the frequency of the wire at different positions relative to the beam. The profile of the laser beam was investigated with VWM at different scan speeds. The energy transferred from the laser, heats up the wire, and shifts the wire tension and therefore the frequency of the wire. The heating of the wire is a dynamic process depending on the experiment conditions (the wire can be placed in air, in other atmosphere, or in the vacuum), wire material, heat transfer mechanism from the measured beam to the wire etc. The important parameter of the profiling process is the response time which depends of the parameters of the VWM and parameters of the atmosphere.

For a triangular temperature profile in the wire, close to the real distribution, the sink of the deposited power via thermal conductivity process is described by the formula:

$$W_{\lambda} = 4(T - T_0)\lambda S / L, \tag{4}$$

where T is maximal temperature of the wire, T_0 is ambient temperature, λ is coefficient of the thermal conductivity, S and L are cross-section and length of the wire, respectively.

To increase the temperature of the wire by mean temperature $(T - T_0)/2$ we need energy

$$E = \frac{T - T_0}{2} c\rho LS \,, \tag{5}$$

where c is specific heat and ρ is density of wire material.

With the assumption that the sink of heat remains the same during the heating process, one can find the time τ_λ required for the transmission the energy to the wire in accordance with formula

$$\tau_\lambda = \frac{c\rho L^2}{8\lambda} \,. \tag{6}$$

In case if thermal sink is produced only by thermal radiation process we have the following formula for radiation power:

$$W_{\mathrm{RAD}} = \varepsilon\sigma_{\mathrm{ST\_B}} T_{\mathrm{MEAN}}^4 \pi dL - \varepsilon\sigma_{\mathrm{ST\_B}} T_0^4 \pi dL \approx 2\varepsilon\sigma_{\mathrm{ST\_B}} T_0^3 (T - T_0)\pi dL \,, \tag{7}$$

where d is the wire diameter, πdL is the wire surface area, and $T_{\mathrm{MEAN}} \approx (T + T_0)/2$ is the wire mean absolute temperature. It is assumed that the wire emissivity ε is the same for thermal emission and deposition. Corresponding response time is obtained by the formula

$$\tau_{\mathrm{RAD}} = \frac{c\rho d}{16\varepsilon\sigma_{\mathrm{ST\_B}} T_0^3} \,. \tag{8}$$

The same procedure was done for convective thermal sink

$$W_{\mathrm{CONV}} = \frac{T - T_0}{2} \alpha_{\mathrm{CONV}} \pi dL \,, \tag{9}$$

where α_{CONV} is coefficient of the convective losses The corresponding response time is

$$\tau_{\mathrm{CONV}} = \frac{c\rho d}{4\alpha_{\mathrm{CONV}}} \,. \tag{10}$$

The final response time τ of all sink mechanisms is obtained by formula

$$1/\tau = 1/\tau_\lambda + 1/\tau_{\mathrm{RAD}} + 1/\tau_{\mathrm{CONV}} \,. \tag{11}$$

As a result, we have

$$\tau = \frac{c\rho}{8(\lambda / L^2 + 2\varepsilon\sigma_{\mathrm{ST\_B}} T_0^3 / d + \alpha_{\mathrm{CONV}} / 2d)} \,. \tag{12}$$

For VWM with stainless steel wire of 0.1 mm diameter and 40 mm length, the convection coefficient is 20 W/m^{2}K, which gives for $\tau \sim 3.9$ s ($\tau_\lambda \approx 48.5$ s, $\tau_{\mathrm{RAD}} \approx 24.7$ s, $\tau_{\mathrm{CONV}} \approx 4.9$ s).

To determine the parameter α_{CONV} we used equation for convection of cylinder moving with speed v in air [18] as

$$\alpha_{\mathrm{CONV}} = 4.13 \frac{v^{0.8}}{d^{0.2}} \,. \tag{13}$$

4. EXPERIMENT

Figure 2 presents the experimental scheme, where for the precise feed of the VWM microscopic stage with micrometric positioning knob was used. This knob was driven by a stepper motor through a belt transmission from the axis of the stepper motor to the knob to reduce the mechanical impact of the stepper

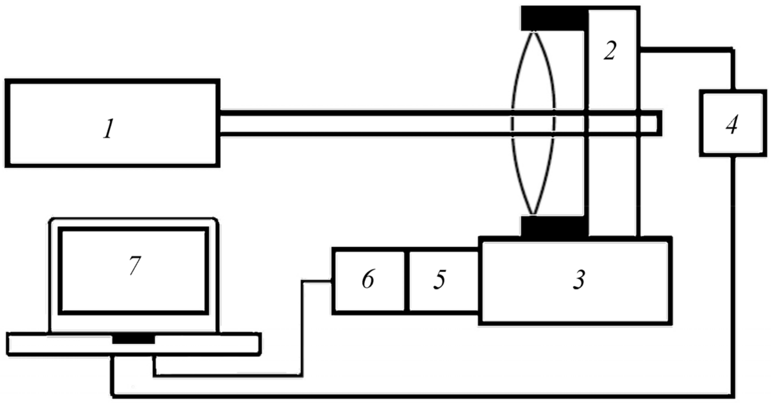

Fig. 2. Scheme of the experiment: *1* − laser, *2* – VWM, *3* − stage with micrometric positioning knob, *4* − VWM electronics with RS232 interface, *5* − stepper motor coupled with stage micrometric positioning knob, *6* − stepper motor electronics with RS232 interface and *7* – computer.

motor bounce on the vibrating wire. The coefficient of steeper motor counts to real feed of VWM was 602 steps/mm. The system had some free running of ~10 μm, which corresponds to 6–7 motor steps.

The scan were prepared by the following scheme: initial 10 s pause, scan of 2000 steps forward at fixed speeds, pause 10 s, and then backward scan to start position.

In this experiment a semiconductor continuous laser was used (Laser point JD-850), with wavelength 532 nm and power 100 mW.

Figure 3 presents the speed of scan is 0.0166 mm/s (10 steps/s). The primary results of the forward and backward scans are presented in Fig. 3a. The gap between the curves is caused by thermal inertia of the wire heating process and the free running in the change of stage movements direction. Figure 3b shows the graphs of forward and backward scans shifted to each other. The value of both shifts is 0.017 mm (10 steps). After this operation the two graphs practically coincide and represent the true profile of the laser beam. The accuracy of the profile recovery can be determined as the difference between the two curves in Fig. 3b. Frequency drop caused by the wire heating is about 68 Hz. The full width at half maximum

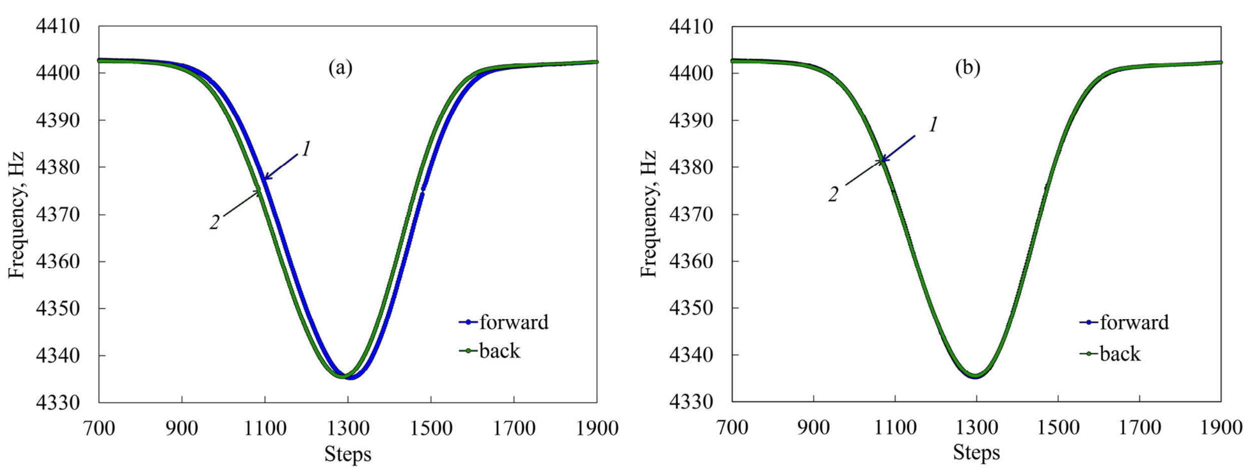

Fig. 3. Scan with the minimal speed of 10 steps/s (0.0166 mm/s): (a) – primary data, (b) – scan graphics are shifted to each other by 10 steps. Curves *1* and *2* are forward and backward scans.

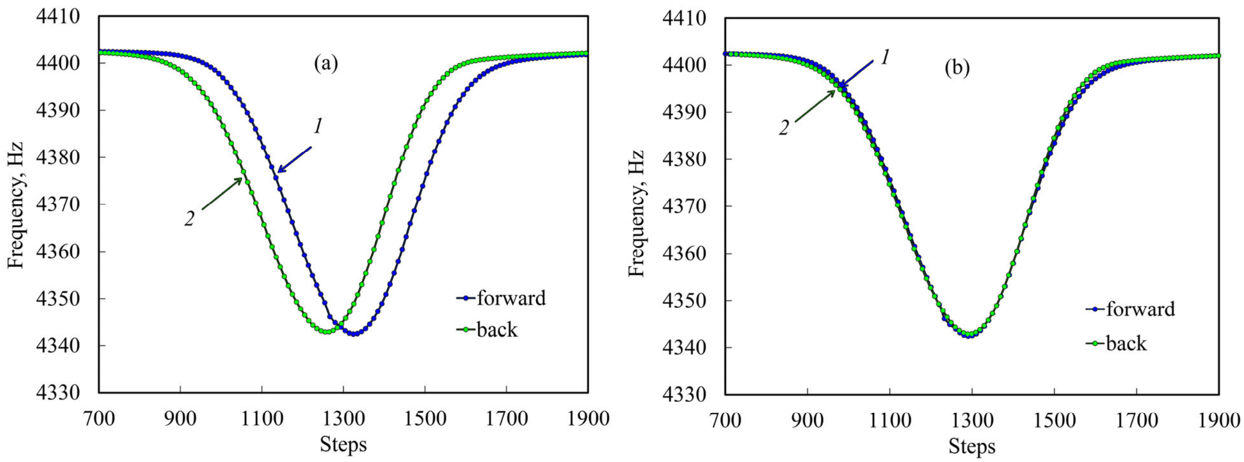

Fig. 4. Scan with the speed of 50 steps/s (0.0830 mm/s): (a) – primary data, (b) – scan graphics are shifted to each other by 34 steps. Curves *1* and *2* are forward and backward scans.

(FWHM) of forward scan is 334.7 steps (0.556 mm). The time of scan is 33.5 s.

Practically the same pattern we see for the speed of scan 0.0332 mm/s (20 steps/s). To overlap the scans from primary data, 0.023 mm (14 steps) shifts were used for each scan. The drop of frequency is 63 Hz, which is less than in previous case. The FWHM of forward scan is 332.8 (0.553 mm) and the time of scan is 16.6 s.

The scans with speed 0.0830 mm/s (50 steps/s) are presented in Fig. 4. Drop of the frequency is ~ 60 Hz. For overlapping of the backward scan with the forward one we used shifts of 0.056 mm (34 steps) toward each other (Fig. 4b). The central parts of the profiles approximately coincide but a small difference arises at the 'tails' of the profiles. This difference is explained by diversity of heating processes at the entrance into the beam and cooling processes at the exit from the beam. The FWHM of forward scan is 340.6 steps (0.566 mm). The time of scan is 6.8 s.

At the speed of scan 0.1661 mm/s (100 steps/s) the drop of frequency is 51 Hz (Fig. 5). The split between the scans shifted by 0.086 mm (52 steps) (Fig. 5b) shows the definitive effect of thermal inertia. The FWHM of forward scan is 362.2 steps (0.602 mm), and the time of scan is 3.6 s.

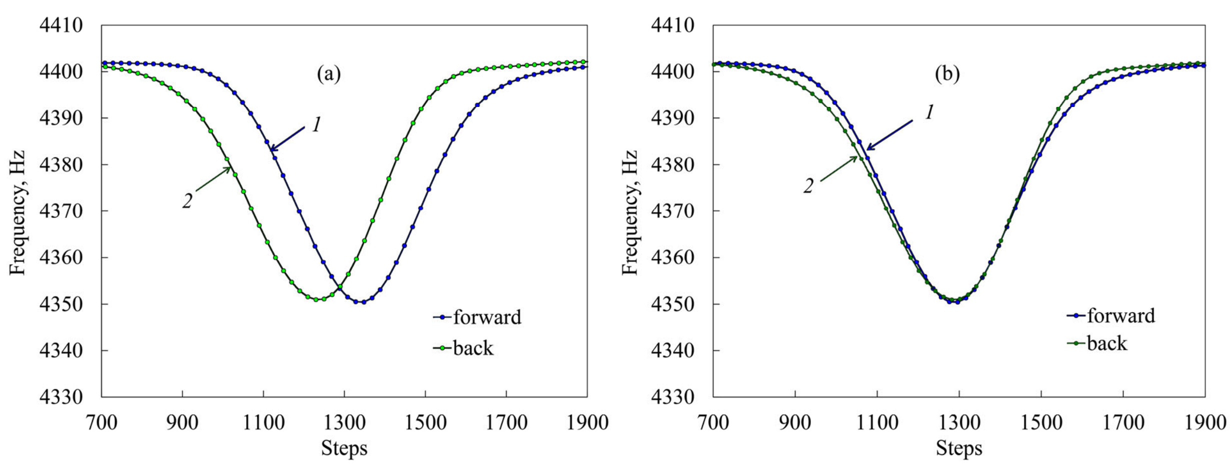

Fig. 5. Scan with the speed of 100 steps/s (0.1661 mm/s): (a) – primary data, (b) – scan graphics are shifted to each other by 52 steps. Curves *1* and *2* are forward and backward scans.

Scan at the speed of 0.2491 mm/s (150 steps/s) with a frequency drop of ~50 Hz was performed. The parameter for shifting the graphs is 0.123 mm (74 steps). The FWHM of forward scan is 398.3 steps (0.622 mm) and the corresponding time is 2.6 s.

The maximal scan speed in the next experiment was 0.3322 mm/s (200 steps/s) with frequency drop of 45 Hz (Fig. 6). The corresponding shifted profiles (by 0.140 mm or 84 steps) coincide near the central part of the profiles while the tail parts remain essentially different. The FWHM of forward scan is 430.2 steps (0.715 mm) and the corresponding time is 2.1 s.

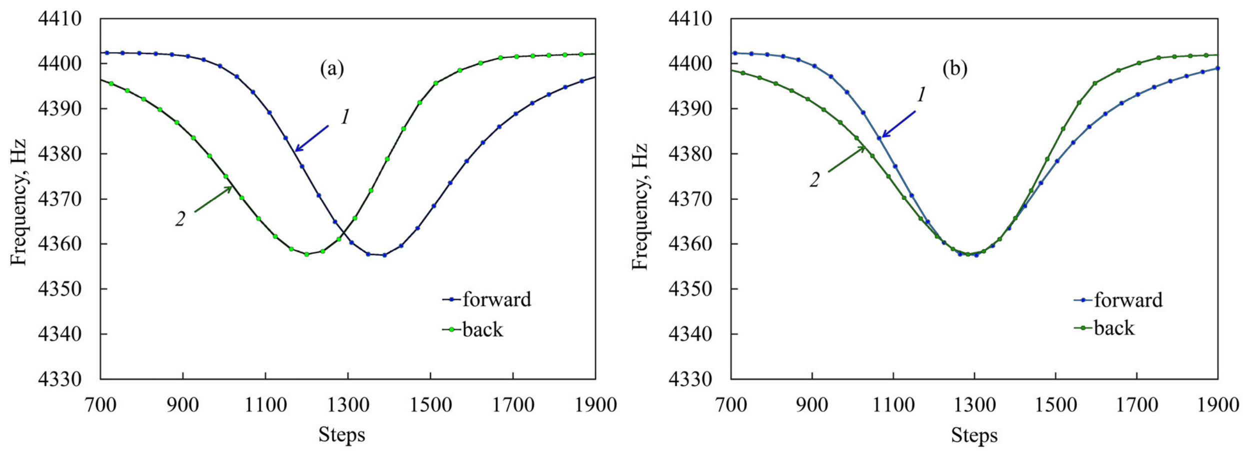

Fig. 6. Scan with the speed of 200 steps/s (0.3322 mm/s): (a) – primary data, (b) – scan graphics are shifted to each other by 84 steps. Curves *1* and *2* are forward and backward scans.

As can be seen from the results of the experiments with increasing scan speed, the number of experimental points on the graphs decreases, and the skewing of the curves relative to the symmetrical profile of the laser beam increases. The VWM response time estimate of 3.9 s gives a qualitative description of the experimental measurements. Indeed, for scan speeds of 0.0166, 0.0332 and 0.0830 mm/s (scan time of 33.5, 16.6, and 6.8 s), the results of forward and backward scans are practically the same. At a speed of 0.1661 mm/s (3.6 s scan time), there is a noticeable diverging between the results of forward and backward scans, which becomes significant at speed of 0.2491 and 0.3322 mm/s. The obtained results suggest to use the comparison of the VWM frequency responses for forward and

Comparative characteristics of forward and backward beam scans at different speeds

Speed, mm/s	FWHM, mm	Time FWHM, s	Number of points	Frequency drop, Hz	Coincidence of the scans, Hz	Profile measurement accuracy, %
0.0166	0.556	33.5	987	68	0.11	0.16
0.0332	0.553	16.6	492	63	0.20	0.32
0.0830	0.566	6.8	194	60	0.42	0.70
0.1661	0.602	3.6	97	51	1.03	2.01
0.2491	0.622	2.6	63	50	2.45	4.89
0.3322	0.715	2.1	48	45	3.22	7.15

backward scans as a measure of the correspondence between the VWM gaugings and real beam profile. For such comparison, we use a simple algorithm based on the calculation of the sum of the absolute distances between frequency data of the VWM, normalized to the number of experimental points.

Since the set of coordinates of the forward and backward scans data along the axis of displacement of the scanner is different, a comparison is made between the chosen experimental point of reverse scan, and the point of direct scan extrapolated linearly between the nearest experimental points of the corresponding curve. The table shows the results of such a procedure performed for all used scan speeds.

The use of forward and backward scans also makes it possible for us to correct the frequency responses of the VWM in order to obtain the real beam profile. Correction is performed by averaging the profiles of forward and backward scans. Figure 7 shows the process of such averaging for the highest scan speed of 0.3322 mm/s. For comparison, the beam profile based on the results of a slow scan is also shown, which is accepted as a reference.

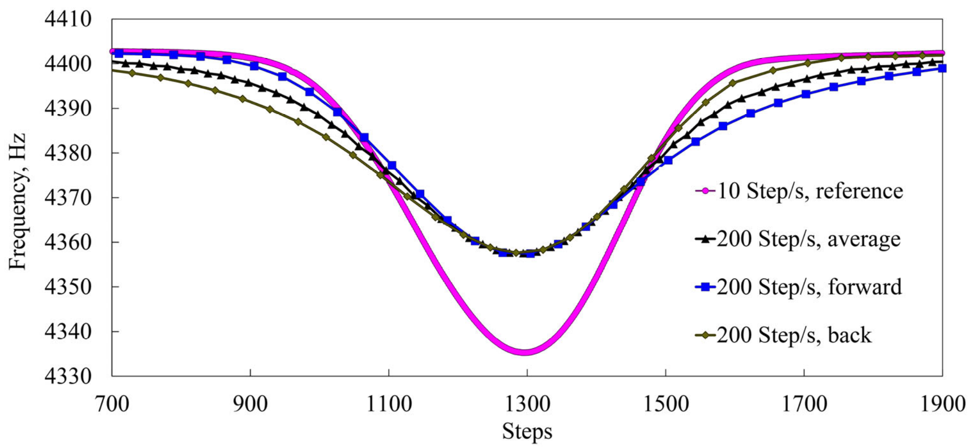

Fig. 7. Graph of averaging (triangles) of forward (squares) and backward (rhombus) scans for a speed of 200 steps/s. The FWHM for this graph is 0.711 mm (428.1 steps). The solid line represents the reference profile, taken at speed of 10 steps/s (FWHM – 0.715 mm).

5. CONCLUSION

The profile of the laser beam was measured by the VWM at different scan speeds. Since the method of the vibrating wire is based on the thermal impact of the beam on the wire, the monitor behaves differently when the wire is heated and cooled, due to the thermal inertia of these processes. To distinguish this difference, a combination of forward and backward scans was used. This method allows to estimate the accuracy of conformity of the frequency signal of the monitor compared to the real beam profile even at high scan speeds (the proper scan speed is determined by comparing the scan time with the characteristic response time of the monitor). The difference between forward and backward scans determines the accuracy of scan at a given speed. The results are used to correct the thermal delay of the frequency response of the VWM.

These results are of interest when using the VWM over a wide range of applications (charged particle, radiation), as they allow to determine the accuracy of the beam profiling and make correction by usage of forward and backward scans at the same speed.

ACKNOWLEDGMENTS

The authors are grateful to R. Reetz and J. Bergoz for their many years support. The authors thank G. Adilkhanyan for valuable assistance in completing the experimental setup. Special thanks to A. Hunanyan for help in the work.

REFERENCES

1. Ageykin, D.I., Kostina, E.N., and Kuznetsova, N.N., *Datchiki kontrolya i regulirovaniya* (Sensors of the Control and Regulation), Moscow: Mashinostroenie, 1965.
2. Asch, G., Andre, P., Beaufront, J., Charnay, G., Cretinon, B., Fouretier, J., Jouvenot, C., Livrozet, P., Mazeran, A., Merigoux, J., Pairot, P., Pligent, J.C., Schon, J.P., Sunyach, M., Tacussel, J., Zelbstein, U., Les Capteurs en Instrumentation Industrielle, Dunod, 1991.
3. Simmonds, T., *Vibrating Wire Tiltmeters and Inclinometers, Recent Developments and Experiences*, Monosys Guide in Monitoring, 2000.
4. Correia da Mata, J.L.G., Fareleria, J.M.N.A., Oliveria, C.M.B.P., and Wakeham, W.A., *A New Instrument to Perform Simultaneous Measurements of Density and Viscosity of Fluids Using a Dual Vibrating-Wire Technique*. – www.zae-bayern.de/ectp/abstracts/correia_da_mata1.html.
5. Krause, A., Erbe, A., and Blick, R.H., *Nanotechnology*, 2000, vol. 11, p. 165.
6. Ayazi, F., Najafi, K., and Harpss, A., *J. Micromechanical Systems*, 2001, vol. 10, p. 169.
7. Arutunian, S.G., Dobrovolski, N.M., Mailian, M.R., Sinenko, I.G., and Vasiniuk, I.E., *Phys. Rev. Special Topics − Accelerators and Beams*, 1999, vol. 2, p. 122801.
8. Arutunian, S.G., Dobrovolski, N.M., Mailian, M.R., and Vasiniuk, I.E., *Phys. Rev. Special Topics − Accelerators and Beams*, 2003, vol. 6, p. 042801.
9. Arutunian, S.G., Mailian, M.R., and Wittenburg, K., *NIM A*, 2007, vol. 572, p. 1022.
10. Tabirian, N., *US Patent 6526077*, 2003.
11. Chung, M., Scarpine, V., Hanna, B., Steimel, J., Shiltsev, V., Arutunian, S.G., and Artinian, S., Transverse Beam Halo Measurements at High Intensity Neutrino Source (HINS) Using Vibrating Wire Method, *Int. Part. Accel. Conf. IPAC2013*, Shanghai, China, 2013, pp. 819−821.
12. Arutunian, S.G., Avetisyan, A.E., Davtyan, M.M., Harutyunyan, G.S., Vasiniuk, I.E., Chung, M., and Scarpine, V., *Phys. Rev. Special Topics − Accelerators and Beams*, 2014, vol. 17, p. 032802.
13. Aginian, M.A., Arutunian, S.G., Cho, D., Chung, M., Harutyunyan, G.S., Kim, S.-Y., Lazareva, E.G., and Margaryan, A.V., *J. Contemp. Phys.* (*Armenian Ac. Sci.*), 2017, vol. 52, p. 110.
14. Arutunian, S.G., *Vibrating Wire Sensors for Beam Instrumentation*, *Beam Instrumentation Workshop*, BIW08, Lake Tahoe, USA, May 4−8, 2008, pp. 1−7.
15. Decker, G., Arutunian, S., Mailian, M., and Rosenbaum, G., *First Vibrating Wire Monitor Measurements of a Hard x-ray Undulator Beam at the Advanced Photon Source*, *Proc. 8th Europ. Workshop on Beam Diagnostics and Instrumentation for Part. Accel. DIPAC2007*, May 20−23, 2007, Venice, pp.36−38.
16. Decker, G., Arutunian, S., Mailian, M., and Vasiniuk, I., *Hard X-ray Synchrotron Measurements at the APS with Vibrating Wire Monitor*, *Beam Instrumentation Workshop, BIW08*, May 4−8, 2008, Lake Tahoe, USA, pp. 36−40.
17. Arutunian, S.G., Bergoz, J., Chung, M., Harutyunyan, G.S., and Lazareva, E.G., *NIM A*, 2015, vol. 797, p. 37.
18. Feuerfestbau, *Werkstoffe-Konstuktion-Ausfuehrung*, Vulkan-Verlag Essenp, 2002.